ISSN 0023-1584, Kinetics and Catalysis, 2007, Vol. 48, No. 3, pp. 448–456. © MAIK "Nauka/Interperiodica" (Russia), 2007.
Original Russian Text © P.V. Snytnikov, A.I. Stadnichenko, G.L. Semin, V.D. Belyaev, A.I. Boronin, V.A. Sobyanin, 2007, published in Kinetika i Kataliz, 2007, Vol. 48, No. 3, pp. 472–480.

Copper–Cerium Oxide Catalysts for the Selective Oxidation of Carbon Monoxide in Hydrogen-Containing Mixtures: II. Physicochemical Characterization of the Catalysts

P. V. Snytnikov[a,b], A. I. Stadnichenko[a], G. L. Semin[a], V. D. Belyaev[a], A. I. Boronin[a,b], and V. A. Sobyanin[a,b]

[a] *Boreskov Institute of Catalysis, Siberian Branch, Russian Academy of Sciences, Novosibirsk, 630090 Russia*
[b] *Novosibirsk State University, Novosibirsk, 630090 Russia*
E-mail: pvsnyt@catalysis.ru
Received February 26, 2006

Abstract—The copper–cerium oxide catalysts were characterized using a set of physicochemical techniques including in situ FTIR spectroscopy, XPS, and XRD. It was found that copper segregated on the surface of cerium oxide and its states were labile and dependent on catalyst pretreatment conditions. Copper in a dispersed state was responsible for the reaction of CO oxidation in the presence of H_2 on the copper–cerium oxide catalysts. It is likely that this state of copper was composed of two-dimensional or three-dimensional surface clusters containing Cu^+ ions.

DOI: 10.1134/S0023158407030147

INTRODUCTION

The copper–cerium oxide system is an active and selective catalyst for the fine purification of hydrogen-containing mixtures to remove CO [1–5]. For example, Avgouropoulos et al. [4] found that the $CuO–CeO_2$ catalyst, whose activity was higher than that of $Pt/\gamma–Al_2O_3$, was considerably superior to the latter in selectivity in gas mixtures that either contained or did not contain water and carbon dioxide. This was due to the fact that carbon monoxide more readily than hydrogen reduced the copper–cerium system. Thus, CO can reduce the copper–cerium oxide catalyst even at room temperature, whereas the reduction with hydrogen came into play only at a temperature higher than 100°C. Previously [2, 3], an attempt was made to find the answers to questions about the structure of active centers in the $CuO–CeO_2$ catalysts and what is responsible for their high activity and selectivity in the reaction of CO oxidation in the presence of hydrogen. For this purpose, a set of physicochemical techniques was used: XRD, XPS, EPR spectroscopy, UV spectroscopy, magnetic measurements, the temperature-programmed reduction (TPR) of samples in hydrogen, etc. It was found that, in the most active $CuO–CeO_2$ catalysts, copper occurred in a highly dispersed state as Cu^{2+} and Cu^+ ions. In particular, both isolated copper ions located in the bulk and on the surface of CeO_2 and species that are more complex (Cu^{2+}–Cu^{2+} dimers and nanosized planar CuO clusters located on the surface of CeO_2) were detected. According to published data [2, 3], the ease of redox processes in these dispersed states of copper is responsible for the high activity and selectivity of $CuO–CeO_2$ catalysts in the oxidation of CO in the presence of H_2. Copper cations participate in the redox equilibrium

$$Ce^{4+} + Cu^+ = Ce^{3+} + Cu^{2+},$$

which is maintained by the presence of these ions in the catalyst even under strongly reducing conditions. In this context, note that, according to Bera et al. [6], the potentials of the redox pairs Cu^{2+}/Cu^+ and Cu^+/Cu^0 in the copper–cerium oxide system are much lower than those in the CuO phase.

The mechanism of CO oxidation in hydrogen-containing mixtures on a copper–cerium oxide catalyst was considered in detail by Sedmak et al. [7]. They studied the reaction kinetics of CO oxidation in the presence of H_2 on the $Cu_{0.1}Ce_{0.9}O_{2-x}$ catalyst; namely, they measured the dependence of the reaction rate of CO oxidation in the presence of H_2 on the partial pressures of O_2 and CO. They found that this dependence was adequately described in terms of a redox mechanism or, what is the same, the Mars–van Krevelen mechanism:

$$(1)\ \text{Cat–O} + \text{Red} \longrightarrow \text{Cat} + \text{Red–O};$$

$$(2)\ \text{Cat} + \text{Ox–O} \longrightarrow \text{Cat–O} + \text{Ox},$$

where steps (1) and (2) reflect the steps of catalyst surface reduction and oxidation, respectively. According to Sedmak et al. [7], highly dispersed copper as cations, which strongly interact with the surface of CeO_2, serve as the active center of $CuO–CeO_2$ catalysts. Taking into account that the redox mechanism is typical of the reactions of separate CO and H_2 oxidation on oxide catalysts, the conclusion that this mechanism also occurs in

the reaction of CO oxidation in the presence of hydrogen on the $CuO–CeO_2$ catalyst seems reasonable.

The first part of our work was devoted to a systematic study of the course of reaction of carbon monoxide oxidation in hydrogen-containing gas mixtures oriented to the determination of conditions for the fine purification of hydrogen to remove CO to a level of 10 ppm [5].

In this part of our work, attention is focused on the physicochemical characterization of oxide copper–cerium catalysts and on the reaction mechanism of CO oxidation in the presence of H_2.

EXPERIMENTAL

The Cu/CeO_{2-x} catalysts were prepared using two methods: coprecipitation and impregnation. The procedures are described in detail elsewhere [5].

The catalysts thus prepared were tested in the reaction of CO oxidation in hydrogen-containing mixtures. A typical reaction mixture consisted of 1 vol % CO + 0.5–1.5 vol % O_2 + 65 vol % H_2 + 20 vol % CO_2 + 10 vol % H_2O + the balance He. The results of the catalytic experiments are also described in detail elsewhere [5].

Methods

The catalysts prepared were characterized using a set of physicochemical techniques.

The concentrations of the main components in the copper–cerium catalysts were determined by inductively coupled plasma atomic emission spectrometry on an Optima instrument from Perkin-Elmer. The analytical procedure involved the dissolution of a solid catalyst sample, the dilution of the resulting solution to a concentration required for spectrometric analysis, and photometric measurements using a calibration graph method.

The specific surface areas (S_{BET}) and pore volumes (V_{pore}) of supports and catalysts were determined from the full isotherms of low-temperature nitrogen adsorption at 77 K, which were measured on an ASAP-2400 instrument (Micrometrics, United States).

The catalysts were studied by transmission electron microscopy on a JEM-2010 electron microscope from JEOL (Japan) at an accelerating voltage of 200 kV. However, this technique did not allow us to identify the microstructures of samples. The resulting micrographs of Cu/CeO_{2-x} catalysts were uniform, and copper was indistinguishable from cerium. This situation was noted previously [8] and explained by the fact that copper is lighter than cerium.

The X-ray diffraction analysis of catalyst samples was performed on a Bruker D-8 diffractometer (CuK_α radiation; graphite monochromator). The measurements were performed by scanning with a step of 0.02 in the angle region $2\theta = 5°–135°$. Data from the JCPDS international diffraction database (PCPDFWIN software) were used as reference standards [9]. The experimental diffraction data were treated using the PowerCel 2.4 program, which allowed us to calculate the quantitative phase composition, the lattice parameters, and the size of coherent-scattering regions (CSRs) of the samples.

The composition and state of catalyst surfaces were studied by X-ray photoelectron spectroscopy (XPS). The XPS spectra were measured on a VG ESCALAB electron spectrometer from VG Scientific (United Kingdom) using AlK_α radiation. The average electron free path (λ) was 20–30 Å depending on the analytical line. The spectra were measured in the retarding potential mode at a constant transmission energy of the hemispherical analyzer. A survey spectrum, which is necessary for obtaining data on the chemical composition of a catalyst surface, was measured at an analyzer transmission energy of 100 eV. In the high-resolution measurements of narrow regions (lines), which are required for obtaining data on the chemical state of an element on the catalyst surface, the analyzer transmission energy was 50 or 20 eV. In the latter case, the line broadening due to the analyzer was 0.3 eV. The treatment of experimental XPS spectra involved several stages; the most important of them are smoothing of curves and background subtraction by the Shirley method [10], deconvolution of spectra [11], and spectral line position calibration. The ratio between component concentrations in a catalyst was determined from the intensities of corresponding XPS lines with consideration for tabulated atomic sensitivity factors [10, 12–14].

To study in greater detail the mechanism of catalytic CO oxidation in hydrogen-containing gas mixtures, kinetic experiments were performed using in situ IR Fourier transform spectroscopy. For this purpose, a heated flow cell (reactor) with an optical path length of 1 mm was made in order to decrease the contribution of CO molecules from a gas phase to the overall spectrum. In this cell, NaCl windows sealed with a high-temperature sealing material were used. The catalyst as a pressed pellet of size 1×2 cm and ~0.1 mm in thickness was placed in the cell. Capillaries introduced into the cell served for the inlet and outlet of a reaction gas mixture. A heating coil and a Chromel–Alumel thermocouple for temperature measurements were mounted outside the cell. The cell was placed in a Shimadzu FTIR-8300 spectrometer. The spectra were measured at a resolution of 4 cm^{-1} with 50 scans per spectrum. The time taken to measure a spectrum was ~1 min. The concentrations of reactants and reaction products at the reactor inlet and outlet were determined using a Kristall 2000 chromatograph (Russia) equipped with a thermal-conductivity detector and a flame-ionization detector with a methanator containing an NKM-4 nickel catalyst. (The chromatographic analysis and the calculation of the conversions of CO and O_2 (X_{CO} and X_{O_2}, respec-

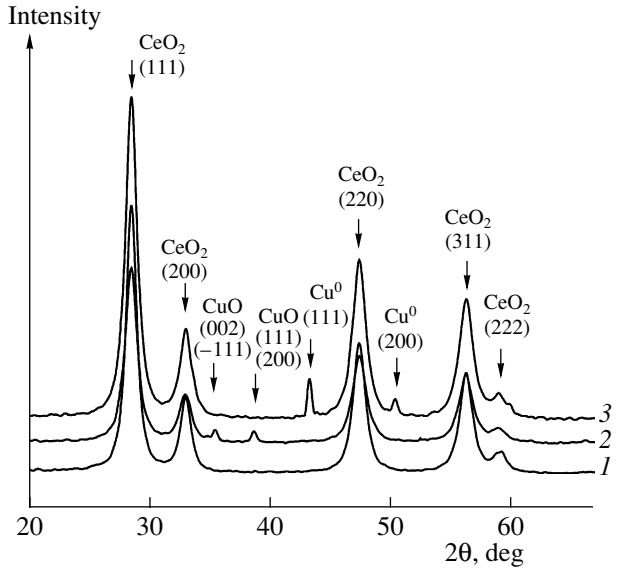

Fig. 1. Diffraction patterns of (*1*) CeO_2 and the CuO/CeO_{2-x}(C) catalyst (*2*) before and (*3*) after the reaction of CO oxidation in hydrogen-containing mixtures.

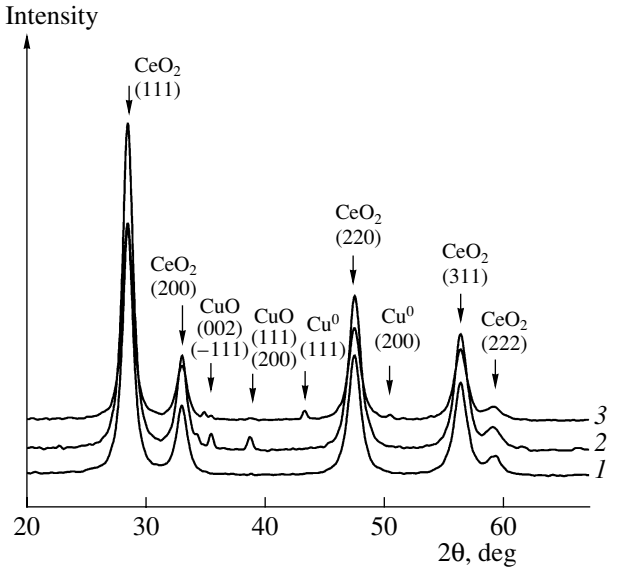

Fig. 2. Diffraction patterns of (*1*) CeO_2 and the CuO/CeO_{2-x}(I) catalyst (*2*) before and (*3*) after the reaction of CO oxidation in hydrogen-containing mixtures.

tively) and selectivity (S) were described in detail elsewhere [5].)

The state of adsorbed CO molecules on catalyst surfaces was monitored using an absorption band in the region 1800–2300 cm^{-1}, which corresponds to the vibrations of CO in complexes with copper [15].

RESULTS AND DISCUSSION

Previously [5], we found that the 14.6 at % Cu/CeO_{2-x} catalyst prepared by impregnation and calcined at 400°C (Cu/CeO_{2-x}(I)) exhibited the highest activity and selectivity toward CO oxidation in hydrogen-containing mixtures. The 14.4 at % Cu/CeO_{2-x} catalyst prepared by coprecipitation and calcined at 400°C (Cu/CeO_{2-x}(C)), which was less active and selective, was used as a reference catalyst. Data on S_{BET} and V_{pore} [5] suggest that the structure of the samples was stable under reaction conditions. A comparison between the physicochemical properties of these catalysts is given below.

The oxide copper–cerium catalysts were studied by XRD analysis. Figures 1 and 2 show the diffraction patterns of CeO_2, which was used for catalyst preparation by the impregnation method, and Cu/CeO_{2-x} catalyst samples before and after the reaction of CO oxidation in the presence of H_2. It can be seen that reflections that correspond to CuO and CeO_2 were observed in both of the oxide copper–cerium catalysts prepared by coprecipitation (Fig. 1, curve *2*) and impregnation (Fig. 2, curve *2*) before the reaction. After the reaction, the CuO phase disappeared from both of the catalysts and a phase of copper metal Cu^0 appeared (Figs. 1, 2, curves *3*). Thus, the catalysts consisted of two phases before and after the reaction: the phases of CeO_2 and CuO were observed before the reaction, whereas the phases of CeO_2 and Cu were observed after the reaction.

Table 1 summarizes the lattice parameters (Δa = ±0.0005 Å) calculated for CeO_2 from the diffraction patterns given in Figs. 1 and 2 and the sizes of coherent-scattering regions for CeO_2, CuO, and Cu in the Cu/CeO_{2-x} catalysts before and after the reaction of CO oxidation in the presence of H_2. It can be seen that, in CeO_2 and both of the catalysts before and after the reaction, the particle sizes of CeO_2 are similar and fall in the range 105–130 Å, as calculated from the sizes of coherent-scattering regions. The particles of CuO in the catalysts before the reaction and Cu in the catalysts after the reaction were much coarser than the particles of cerium oxide, and their particle size was ~500–1000 Å.

Table 1 also summarizes the calculated phase compositions of the catalysts. The amounts of individual phases in the copper–cerium oxide catalysts (in at %) were determined using the equation $100N'_{Cu}/(N_{Cu} + N_{Ce})$, where N_{Ce} and N_{Cu} are the known numbers of cerium and copper atoms, respectively, in the weighed portions of catalyst samples, and N'_{Cu} is the number of copper atoms in a CuO or Cu phase, which was obtained by calculating the weight content from the above diffraction patterns. It can be seen that, in the Cu/CeO_{2-x}(C) catalyst, the amount of copper introduced was 14.4 at %; in this case, the major portion of copper in the catalyst before the reaction occurred as a CuO phase (11.6 at %). In the catalyst prepared by impregnation, the amount of copper introduced was 14.6 at % and only 7.4 at % copper occurred as a CuO phase before the reaction.

Table 1. XRD data for copper–cerium catalysts

Catalyst	Phase composition, at %		Unit cell parameter a_{CeO_2}, Å	CSR D_{CeO_2}, Å	CSR D_{Cu}, Å	CSR D_{CuO}, Å
	CuO	Cu				
CeO_2	–	–	5.4162*	117–121	–	–
14.4 at % Cu/CeO_{2-x}(C) coprecipitation, before reaction	11.6	–	5.4114	105–110	–	500–1000
14.4 at % Cu/CeO_{2-x}(C) coprecipitation, after reaction	–	9.6	5.4146	115–119	500–1000	–
14.6 at % Cu/CeO_{2-x}(I) impregnation, before reaction	7.4	–	5.4112	125–130	–	500–1000
14.6 at % Cu/CeO_{2-x}(I) impregnation, after reaction	–	4.2	5.4144	125–130	500–1000	–

* The unit cell parameter of CeO_2 is consistent with reference data for CeO_2 in the JCPDS database.

The CuO phase fully disappeared from both of the catalyst samples after the reaction of CO oxidation in the presence of H_2, and a copper metal phase appeared in concentrations of 9.6 and 4.2 at % for the coprecipitated and impregnated samples, respectively. The experimental data indicate that a portion of copper introduced into the catalysts was not detected by XRD. This is likely due to the fact that copper occurred in the catalysts in a dispersed state, as isolated ions incorporated into the lattice of CeO_2, or as nanostructures arranged on the surface of CeO_2. This hypothesis is based on the fact that, both before and after the reaction, the lattice parameter of CeO_2 was smaller by 0.002–0.005 Å than the parameter of pure cerium oxide (see Table 1). These results are consistent with data published by Liu et al. [16, 17], who related the observed decrease in the CeO_2 lattice parameter in oxide copper–cerium systems to the fact that Cu^+ ions are incorporated into the lattice of cerium oxide.

According to XRD data, the amount of copper in a dispersed state in the catalyst prepared by impregnation was much greater than that in the catalyst prepared by coprecipitation.

The state of copper in the Cu/CeO_{2-x} catalysts was determined by XPS. The calibration of XPS spectra was performed using the Ce $3d(u''')$ line, E_b = 917 eV. An analysis of the electronic states of copper and cerium in the Cu/CeO_{2-x} catalysts prepared by both of the methods either before or after the reaction of CO oxidation in the presence of H_2 was performed using Cu $2p_{3/2}$ and Ce $3d$ lines [18–23]. Figures 3–6 and Table 2 summarize the results. Let us consider these results in more detail.

Table 2 indicates that the amount of copper on a catalyst surface was much higher than that in the bulk in all of the catalyst samples. This suggests that copper is segregated on the surface of cerium oxide.

As can be seen in Fig. 3, the Cu $2p$ XPS spectrum of the freshly prepared (before reaction) Cu/CeO_{2-x}(C) catalyst was characterized by a line at E_b(Cu $2p_{3/2}$) = 933.1 eV and a shake-up satellite at E_b = 941.6 eV, which unambiguously suggests the occurrence of Cu^{2+} in the catalyst [18]. The ratio between the areas of the Cu $2p_{3/2}$main peak and the shake-up satellite suggests that only ~67% of the total copper in the catalyst occurred as Cu^{2+}, and the rest of copper occurred as Cu^+.

The Cu $2p$ XPS spectrum of the freshly prepared (before reaction) Cu/CeO_{2-x}(I) catalyst was also characterized by a line at E_b(Cu $2p_{3/2}$) = 933.0 eV and a shake-up satellite with E_b = 941.9 eV. The ratio between the areas of the Cu $2p_{3/2}$ main peak and the shake-up satellite suggests that only ~37% copper in the catalyst occurred in the oxidation state Cu^{2+}. The rest of the copper occurred in the state Cu^+. Note that the presence of Cu^+ and Cu^{2+} in copper–cerium catalysts prepared by various methods was observed previously [2, 3, 8].

Comparing these data and the XRD data, we can conclude that a considerable portion of introduced copper occurred as a CuO phase in the catalysts prepared by coprecipitation and impregnation before the reaction. The rest of the copper, which cannot be detected by XRD analysis, occurred in a finely dispersed state primarily as Cu^+. Both XRD analysis and XPS demonstrated that the amount of copper in the dispersed state

Table 2. XPS data for Cu/CeO_{2-x} catalysts

Catalyst	Surface Cu/Ce atomic ratio
14.4 at % Cu/CeO_{2-x} (coprecipitation, before reaction)	1.7
14.4 at % Cu/CeO_{2-x} (coprecipitation, after reaction)	0.75
14.6 at % Cu/CeO_{2-x} (impregnation, before reaction)	1.43
14.6 at % Cu/CeO_{2-x} (impregnation, after reaction)	1.41

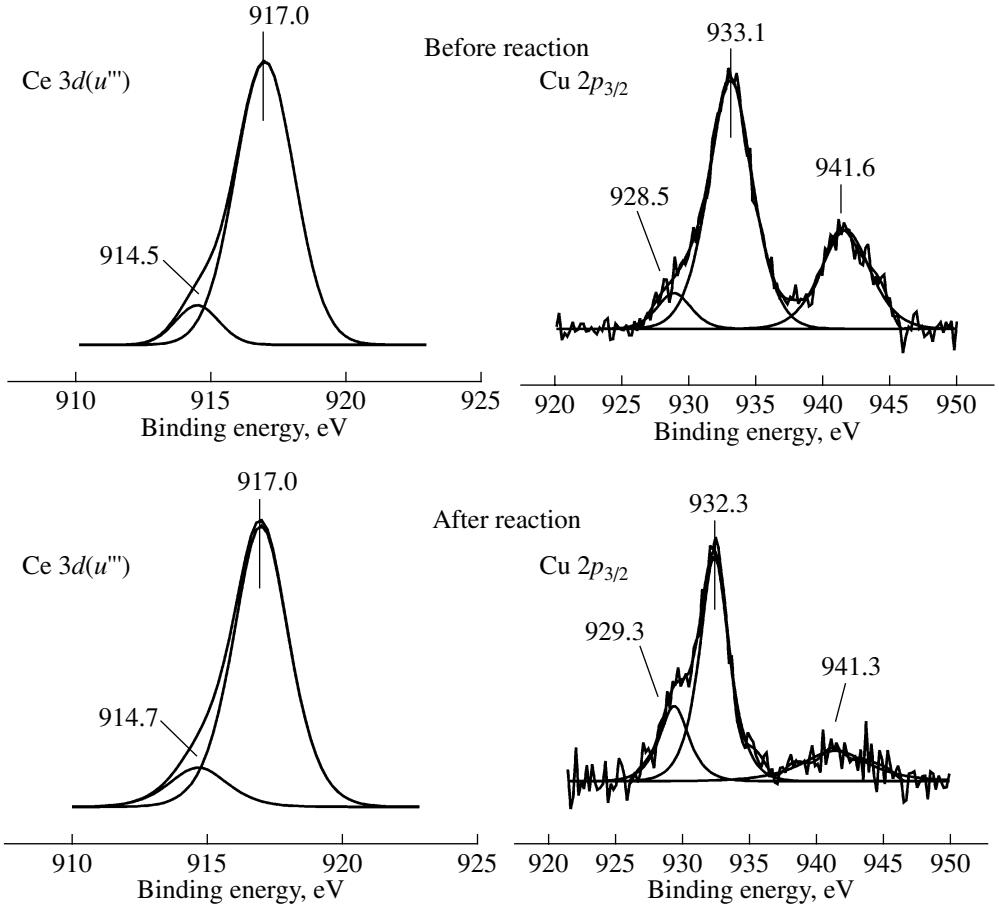

Fig. 3. Cu $2p_{3/2}$ and Ce $3d(u''')$ XPS spectra of the CuO/CeO_{2-x}(C) catalyst before and after the reaction of CO oxidation in hydrogen-containing gas mixtures.

in the catalyst prepared by impregnation was higher than that in the coprecipitated catalyst.

The Cu 2*p* XPS spectrum of the coprecipitated catalyst after the reaction (Fig. 3) exhibited a shift of the Cu $2p_{3/2}$ main peak (E_b = 932.3 eV) toward low values of E_b and a decrease in the peak area of a shake-up satellite. This suggests the partial reduction of Cu^{2+} to Cu^+ or Cu^0. Unfortunately, they cannot be unambiguously identified by XPS because of similar binding energies of the Cu $2p_{3/2}$ lines for the copper states Cu^+ and Cu^0.

The Cu 2*p* XPS spectrum of the impregnated catalyst after the reaction of CO oxidation in the presence of H_2 (Fig. 4) also exhibited a shift of the Cu $2p_{3/2}$ main peak (E_b = 932.7 eV) toward low values of E_b and the disappearance of a shake-up satellite peak. This suggests the complete reduction of Cu^{2+} to Cu^+ or Cu^0.

Comparing the XPS and XRD data for both of the catalysts after the reaction of CO oxidation in the presence of H_2, we can conclude that copper, which occurred as CuO in the samples before the reaction, was reduced to copper metal.

As can be seen in Figs. 3 and 4, the Cu $2p_{3/2}$ lines in the spectra of the catalysts before and after the reaction exhibited a shoulder on the side of lower binding energies. The deconvolution of the Cu $2p_{3/2}$ line into two peaks demonstrated that the shoulder had an anomalously low value of E_b(Cu $2p_{3/2}$) = 928.5–929.7 eV for the 2*p* level of copper in well-known oxidation states [12, 14, 18]. Liu and Flytzani-Stephanopoulos [8] found the presence of this line, which was attributed to isolated Cu^{2+} ions; in our opinion, this assignment is incorrect. It is likely that the line at the abnormally low E_b(Cu $2p_{3/2}$) = 928.5–929.7 eV was due to a differential charging effect in different phases of a sample in the course of measuring photoelectron spectra. We believe that, in the Cu/CeO_{2-x} catalysts, copper is distributed over two phases with different conductivities. As follows from the above XRD data, these phases are CuO or Cu bulk phases and a dispersed phase of copper, which strongly interacts with the surface of cerium oxide. If this is the case, the Ce $3d(u''')$ XPS spectrum will also exhibit an anomaly. To test this hypothesis, we performed the deconvolution of the Ce $3d(u''')$ component, which is shown in Figs. 3 and 4, into constituent peaks. It can be seen that the Ce $3d(u''')$ line also consists of two peaks: the main peak at E_b(Ce $3d(u''')$) = 917.0 eV, which is characteristic of CeO_2, and a weak

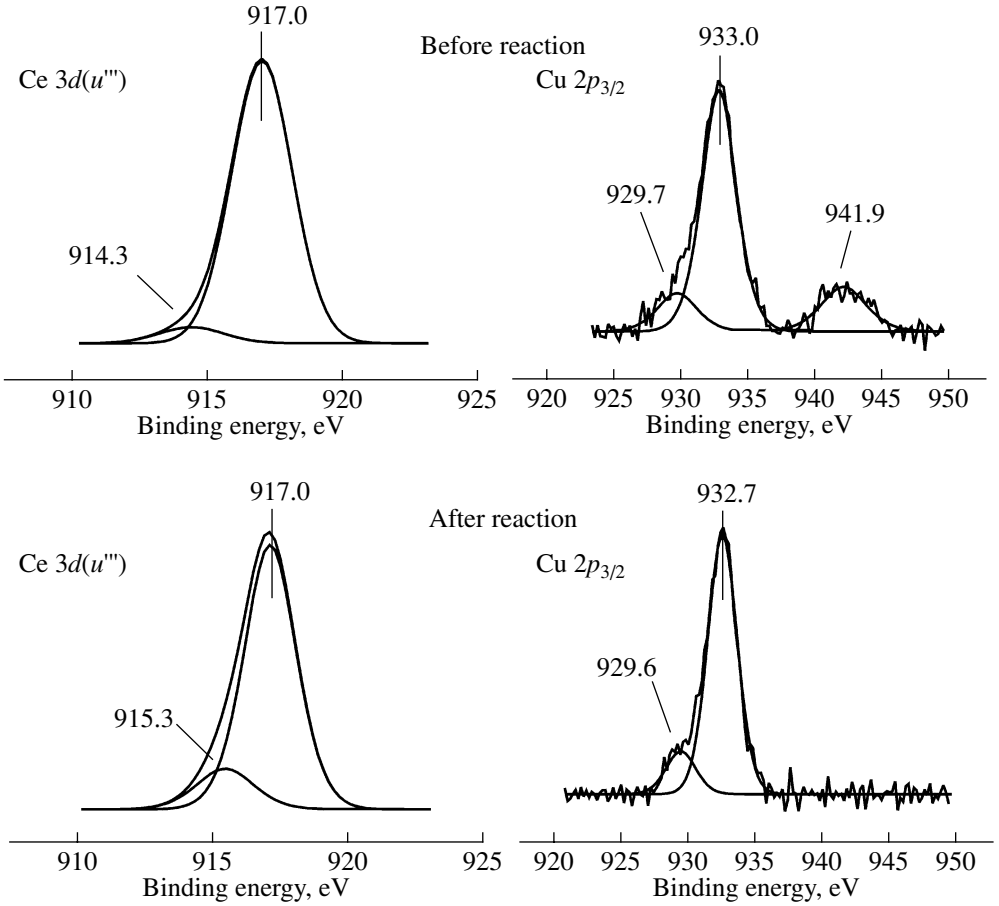

Fig. 4. Cu $2p_{3/2}$ and Ce $3d(u''')$ XPS spectra of the CuO/CeO_{2-x}(I) catalyst before and after the reaction of CO oxidation in hydrogen-containing gas mixtures.

peak at an anomalously low value of binding energy E_b(Ce $3d(u''')$) = 914.3–915.3 eV. Evidently, these anomalies in the Cu $2p$ and Ce $3d$ spectra of the Cu/CeO_{2-x} system are due to a differential charging effect; it is likely that they characterize dispersed copper, which strongly interacts with the surface of CeO_2. This was supported by XRD data, according to which the lattice parameter of cerium oxide was changed upon the introduction of copper (see above).

Figures 5 and 6 compare the full Ce $3d$ XPS spectra of CeO_2 and Cu/CeO_{2-x} catalyst samples before and after the reaction of CO oxidation in the presence of H_2. It can be seen (Fig. 5) that the spectra of CeO_2 and the coprecipitated catalyst before and after the reaction exhibited lines characteristic of Ce^{3+} at E_b(Ce $3d(u')$) = 905 eV and E_b(Ce$3d_{5/2}(v')$) = 885 eV (they are indicated with arrows in Figs. 5, 6) in addition to lines characteristic of Ce^{4+}. This suggests that the surface concentration of Ce^{3+} was significant in the coprecipitated catalyst. At the same time, in the Ce $3d$ XPS spectra of the impregnation catalyst both before and after the reaction, the line intensity of Ce^{3+} was much lower than that in CeO_2 (Fig. 6). This fact suggests that the surface concentration of Ce^{3+} in this catalyst was lower than that in CeO_2.

Based on these results and the results obtained by XRD analysis, we can conclude that cerium oxide interacted with supported copper in the Cu/CeO_{2-x}(I)

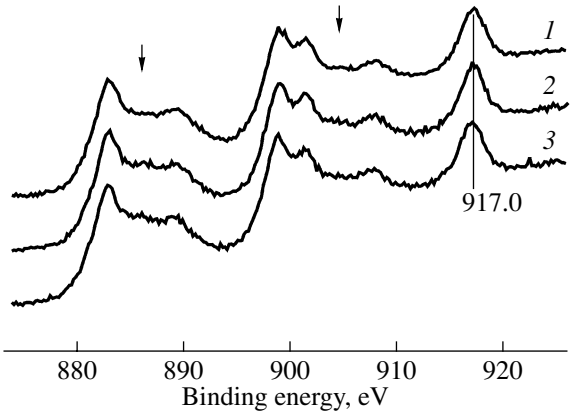

Fig. 5. Ce $3d$ XPS spectra of (*1*) CeO_2 and the CuO/CeO_{2-x}(C) catalyst (*2*) before and (*3*) after the reaction of CO oxidation in hydrogen-containing gas mixtures.

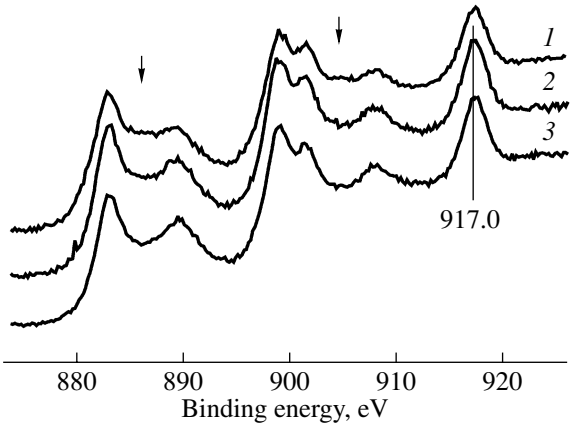

Fig. 6. Ce 3*d* XPS spectra of (*1*) CeO_2 and the CuO/CeO_{2-x}(I) catalyst (*2*) before and (*3*) after the reaction of CO oxidation in hydrogen-containing gas mixtures.

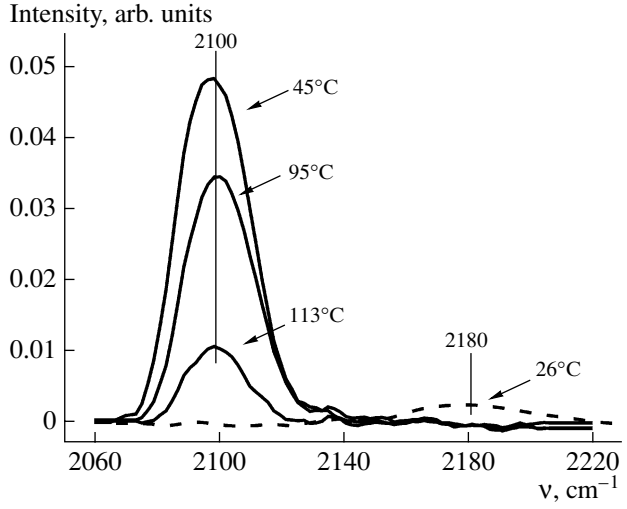

Fig. 7. IR Fourier transform spectra of CO measured in situ in the course of CO oxidation in the presence of H_2 on the CuO/CeO_{2-x}(I) catalyst. Initial gas mixture: 0.7 vol % CO, 0.7 vol % O_2, 50 vol % H_2, and the balance He. Space velocity: 10000 h^{-1}.

catalyst. By analogy with published data [7], we believe that the following redox reaction can occur on the surface even in the course of catalyst preparation:

$$Ce^{3+} + Cu^{2+} = Ce^{4+} + Cu^{+}.$$

To determine the state of copper in a copper–cerium oxide catalyst in the course of CO oxidation in the presence of H_2, we were the first to perform in situ experiments with the use of IR Fourier transform spectroscopy. As an example, Fig. 7 shows the IR spectra of adsorbed CO molecules measured in the course of the CO oxidation reaction in the presence of H_2 at various temperatures on the Cu/CeO_{2-x}(I) catalyst. The temperature dependence of the conversions of CO and O_2 and selectivity in the experiments performed in a heated IR flow cell was similar to the dependence obtained in an ordinary reactor [5]. We found that a small peak with a maximum at 2180 cm^{-1} appeared upon the supply of a reaction mixture (0.7 vol % CO, 0.7 vol % O_2, 50 vol % H_2, and the balance He; space velocity, 10000 h^{-1}) to the catalyst at room temperature. However, even a small increase in the temperature caused a rapid decrease in the intensity of this peak, and a peak with a maximum at 2100 cm^{-1} appeared. To interpret the experimental spectra, we used data published by Tikhov et al. [15], who studied copper-containing catalysts supported on aluminum oxide. It was found that the absorption band at 2180 cm^{-1} corresponds to the vibrations of CO molecules adsorbed at Cu^{2+} ions as the constituents of copper(II) oxide; absorption bands at 2080 and 2140 cm^{-1} are characteristic of CO molecules adsorbed at copper metal and Cu^{+} ions as the constituents of copper(I) oxide, respectively. The absorption band at 2100 cm^{-1} corresponds to the vibrations of CO molecules adsorbed at reduced two-dimensional and three-dimensional copper clusters, which are arranged on the surface of the oxide support. Based on these results, we attributed the absorption bands at 2180 and 2100 cm^{-1} to the vibrations of CO molecules adsorbed at Cu^{2+} ions and reduced two-dimensional and three-dimensional copper clusters on the surface of cerium oxide, respectively. Recently, Manzoli et al. [24], who measured the IR spectra of CO adsorbed on the 5 wt % Cu/CeO_2 catalyst at a low temperature (90 K), proposed an analogous interpretation. They also assigned the peaks at 2180–2140 cm^{-1} to the vibrations of CO molecules adsorbed on copper oxides and the peak at 2097 cm^{-1} to the vibrations of CO adsorbed on copper clusters. This is a serious argument for the fact that the peak with a maximum at 2100 cm^{-1} observed in our experiments corresponds to the vibrations of CO molecules adsorbed at copper clusters on the surface of cerium oxide. Thus, we can conclude that the reduction of supported copper in copper–cerium oxide catalysts in a reactive atmosphere occurred even at room temperature.

As can be seen in Fig. 7, the peak intensity at 2100 cm^{-1} decreased with the reaction temperature. At temperatures higher than 150°C, the peak intensity was close to zero. In a repeated experiment with the same catalyst sample at room temperature, only a maximum at 2100 cm^{-1} was observed.

Analogous results were obtained with the coprecipitated catalyst. This suggests that the reaction of CO oxidation in the presence of H_2 on the Cu/CeO_{2-x} catalysts prepared by impregnation and coprecipitation occurred by the same mechanism. However, the intensities of peaks observed in the IR spectra were lower by an order of magnitude and, correspondingly, the amount of highly dispersed copper that occurred as surface clusters in the coprecipitated catalyst was much smaller than that in the catalyst prepared by impregnation.

Summarizing the experimental data, we can conclude that copper is segregated on the surface of cerium dioxide; its states are labile and dependent on pretreatment conditions. In the catalysts prepared by both impregnation and coprecipitation, a portion of copper occurred as coarse CuO particles before the reaction. These particles were reduced to copper metal in the course of the reaction; it is likely that they did not participate in the reaction. The rest of the copper in these catalysts occurred in a finely dispersed state on the surface of cerium dioxide (as two-dimensional or three-dimensional clusters containing Cu^+ ions). The amount of dispersed copper in the impregnation catalyst was much larger than that in the coprecipitated catalyst.

Previously [5], we found that the prepared oxide copper–cerium catalysts and copper–cerium oxide catalysts described in the literature [1, 25] are similar in both activity and selectivity in the reaction of CO oxidation in hydrogen-containing mixtures.

Based on XRD and XPS data, Sedmak et al. [7] believed that highly dispersed copper as cations, which strongly interact with the surface of CeO_2, serves as active centers in copper–cerium oxide catalysts. The results of our XRD and XPS studies allowed us to conclude that, indeed, the reaction of CO oxidation in the presence of H_2 on copper–cerium oxide catalysts occurred with the participation of finely dispersed copper. Moreover, using in situ IR spectroscopy, we found that finely dispersed copper occurs as two-dimensional and three-dimensional clusters containing cationic copper Cu^+.

Thus, the copper–cerium oxide catalysts studied in this work and described in the literature are similar in not only activity and selectivity but also physicochemical characteristics. This is a serious argument in favor of the similarity between the reaction mechanisms of CO oxidation in the presence of H_2 on the prepared copper–cerium oxide catalysts and the catalysts proposed in the literature. In accordance with published data, cerium oxide actively interacts with supported copper. Because the ionic radii of Cu^+ and Ce^{4+} are similar, copper can be readily incorporated into the lattice of cerium oxide. On the one hand, this allows one to stabilize Cu^+ in a reducing atmosphere in the removal of CO from hydrogen-containing mixtures. On the other hand, oxygen vacancies are formed because of the replacement of the Ce^{4+} ion by the Cu^+ ion with a smaller charge; this is the reason for the higher mobility of oxygen in the catalyst lattice and, correspondingly, the high reactivity of the copper–cerium oxide catalyst. We are prone to adhere to this conclusion.

Thus, based on the well-known published data and the results obtained in this work, we believe that the reaction of CO oxidation in the presence of H_2 occurs by the Mars–van Krevelen redox mechanism as follows: CO is adsorbed at Cu^+ cations, which occur on the catalyst surface as copper clusters. Then, the adsorbed CO molecules are oxidized by the lattice oxygen of the catalyst to CO_2. The catalyst surface is oxidized either directly by gas-phase oxygen or by the lattice oxygen of CeO_2. The oxidation of hydrogen also occurs by this mechanism on copper–cerium clusters. However, because the activity of the copper–cerium oxide system in the oxidation of carbon monoxide is higher than that in the oxidation of hydrogen [5], almost 100% selectivity was reached on the Cu/CeO_{2-x} catalyst.

ACKNOWLEDGMENTS

We are grateful to Dr. Sci. (Chem.) L.M. Plyasova for performing XRD analysis and to Dr. Sci. (Chem.) E.A. Paukshtis for his assistance in IR spectroscopic measurements.

This work was supported in part by the Federal Agency for Science and Innovations within the framework of the Federal Special Scientific and Technical Program "Research and Development in Priority Areas of Science and Technology" (2006-RI-19.0/001/0.15).

REFERENCES

1. Avgouropoulos, G., Ioannides, T., Matralis, H.K., Batista, J., and Hocevar, S., *Catal. Lett.*, 2001, vol. 73, p. 33.
2. Ratnasamy, P., Srinivas, D., Satyanarayana, C.V.V., Manikandan, P., Senthil Kumaran, R.S., Sachin, M., and Shetti, V.N., *J. Catal.*, 2004, vol. 221, p. 455.
3. Avgouropoulos, G. and Ioannides, T., *Appl. Catal., A*, 2003, vol. 244, p. 155.
4. Avgouropoulos, G., Ionnides, T., Papadopolou, C., Batista, J., Hocevar, S., and Matralis, H.K., *Catal. Today*, 2002, vol. 75, p. 157.
5. Snytnikov, P.V., Stadnichenko, A.I., Semin, G.L., Belyaev, V.D., Boronin, A.I., and Sobyanin, V.A., *Kinet. Katal.*, 2007, vol. 48, no. 3, p. 463 [*Kinet. Catal.* (Engl. Transl.), vol. 48, no. 3, p. 439].
6. Bera, P., Mitra, S., Sampath, S., and Hegde, M.S., *Chem. Commun.*, 2001, vol. 10, p. 927.
7. Sedmak, G., Hocevar, S., and Levec, J., *J. Catal.*, 2003, vol. 213, p. 135.
8. Liu, W. and Flytzani-Stephanopoulos, M., *J. Catal.*, 1995, vol. 153, p. 317.
9. *Powder Diffraction File, Alphabetical Index, Inorganic Phases*, Swarthmore, Pa: Joint Committee on Powder Diffraction Standards, 1983, p. 1023.
10. *Practical Surface Analysis by Auger and X-ray Photoelectron Spectroscopy*, Briggs, D. and Seah, M.P., Chichester: Wiley, 1983.
11. Boronin, A.I., *Doctoral (Chem.) Dissertation*, Novosibirsk: Inst. of Catalysis, 2002.
12. Moulder, J.F., Stickle, W.F., Sobol, P.E., and Bomben, K.D., *Handbook of X-ray Photoelectron Spectroscopy*, Eden Prairie, Minn.: Perkin-Elmer, 1992.
13. Nefedov, V.N., *Rentgenoelektronnaya spektroskopiya khimicheskikh soedinenii* (X-ray Photoelectron Spectroscopy of Chemical Compounds), Moscow: Khimiya, 1984.

14. *NIST X-ray Photoelectron Spectroscopy Database*, 1997.
15. Tikhov, S.F., Sadykov, V.A., Kryukova, G.N., Paukshtis, E.A., Popovskii, V.V., Starostina, T.G., Kharlamov, G.V., Anufrienko, V.F., Poluboyarov, V.F., Razdobarov, V.A., Bulgakov, N.N., and Kalinkin, A.V., *J. Catal.*, 1992, vol. 134, p. 506.
16. Liu, Y., Nayakawa, T., Suzuki, K., and Hamakawa, S., *Catal. Commun.*, 2001, vol. 2, p. 195.
17. Liu, W. and Flytzani-Stephanopoulos, M., *J. Catal.*, 1995, vol. 153, p. 304.
18. Schon, G., *Surf. Sci.*, 1973, vol. 35, p. 96.
19. Wong, G.S. and Vohs, J.M., *Surf. Sci.*, 2002, vol. 498, p. 266.
20. Holgado, J.P., Munuera, G., Espinos, J.P., and Gonzalez-Elipe, A.R., *Appl. Surf. Sci.*, 2000, vol. 158, p. 164.
21. Holgado, J.P., Alvarez, R., and Munuera, G., *Appl. Surf. Sci.*, 2000, vol. 161, p. 301.
22. Pflau, A. and Schiefbaum, K.D., *Surf. Sci.*, 1994, vol. 321, p. 71.
23. Ceaser, D.A. and Harrison, P.G., *Catal. Lett.*, 1994, vol. 23, p. 13.
24. Manzoli, M., Monte, R.D., Boccuzzi, F., Coluccia, S., and Kaspar, J., *Appl. Catal., B*, 2005, vol. 61, p. 192.
25. Kim, D.H. and Cha, J.E., *Catal. Lett.*, 2003, vol. 86, nos. 1–3, p. 107.